Front. Optoelectron.
DOI 10.1007/s12200-015-0523-x

RESEARCH ARTICLE

Effect of excitation frequency on characteristics of mixture discharge in fast-axial-flow radio frequency-excited carbon dioxide laser

Heng ZHAO, Bo LI, Wenjin WANG, Yi HU, Youqing WANG (✉)

School of Optical and Electronic Information, Huazhong University of Science and Technology, Wuhan 430074, china

Abstract A one-dimensional fluid model has been used to describe the effect of radio frequency (RF) on the characteristics of carbon dioxide (CO_2), nitrogen (N_2) and helium (He) mixture discharge at 120 mbar in fast-axial-flow RF-excited CO_2 laser. A finite difference method was applied to solve the one-dimensional fluid model. The simulation results show that the spatial distributions of electron density and current density rely strongly on the modulating driven frequency. When the excitation frequency changes from 5 to 45 MHz, the plasma discharge is always in α mode. Moreover, as the excitation frequency increasing, the higher densities of CO_2^{V001} and N_2^{*Vib} can be obtained, which is important to get higher excitation efficiency for the upper laser level.

Keywords plasma, numerical simulation, $CO_2/He/N_2$ mixture discharges, one-dimensional fluid model

1 Introduction

The fast-axial-flow radio frequency (RF)-excited CO_2 laser finds applications in current research areas like nano-particle synthesis, generation of mono-energetic million electron volts (MeV) photons in laser synchrotron sources and 13.5 nm extreme ultraviolet (EUV) sources for the next generation high volume chip manufacturing, particle acceleration, etc. [1–8]. The main reaction gases in fast-axial-flow RF-excited CO_2 laser contain CO_2, nitrogen (N_2) and helium (He). In those main reaction gases, CO_2 molecules are excited to typically emit photons at a wavelength of 10.6 μm. N_2 molecules are excited by the discharge into a meta-stable vibrational level and transfer their excitation energy to the CO_2 molecules when colliding with them. He serves to depopulate the lower laser level and to remove the heat. The performance of high-power fast-axial-flow RF-excited CO_2 laser is directly determined by the stable glow discharge of RF gas mixture in discharge tube. The stable gas discharge is influenced by discharge gap distance, gas mixture ratio, excitation frequency, excitation voltage, and so on. In the $CO_2/He/N_2$ mixture discharge, the density distributions of individual species and characteristics of the discharge modes under different frequencies are not well understood yet. In this paper, the stable gas discharge versus the excitation frequency are investigated.

To research the influence of excitation frequency in the stable gas discharge in RF excitation of CO_2 laser, various discharge models and simulations have been studied in recent years In 1991, Wester and Seiwert [9] proposed that as the excitation frequency increased, the excitation efficiency of RF excited CO_2 laser gets increased. However, their study did not give much insight into the relationship among electron density, electric field, and excitation frequency. Then, Wang et al. [10]. used energy balance equation and electron density balance equation to describe distributions of electron density and electric field in coaxial CO_2 laser under 27.12 and 54.24 MHz. In 2007, Zhang et al. [11] presented the spatial distributions of electron density, electric field, and electron energy in different excitation frequencies in slab oxygen iodine laser.

Their calculation revealed that along with the augment of excitation frequency, the relative electric field decreased and electron density increased.

However, they did not explain in detail the relationship between discharge model and excitation frequency. In order to systematically research the influence of excitation frequency in the stable gas discharge in fast-axial-flow RF-excited CO_2 laser, CO_2, N_2 and He have been used as

Received April 8, 2015; accepted July 8, 2015

E-mail: yqwang13@163.com

reaction gases to simulate gas mixture discharge at 120 mbar under different frequencies.

The research only study on the influence of excitation frequency to the $CO_2/He/N_2$ mixture discharge, the other variation of index does not count into the consideration. So, this study used a fluid model to numerically simulate this discharge and the calculations results on the distributions of electron density, current density, electric field, electron temperature, and electron production rate along with the variation of excitation frequency in the discharge gas mixture. Some experimental results [12–14] can be explained well by this numerical simulation.

2 Simulation models

Figure 1 shows the geometry of the planar discharge structure. The discharge of CO_2, N_2, and He mixture is generated between two parallel electrodes and insulators with a RF excitation voltage. In this study, a one-dimensional (1D) self-consistent fluid simulation on $CO_2/He/N_2$ mixture discharge at 120 mbar was performed. The 1D self-consistent fluid simulation of glow discharge was founded by Lymberopoulos and Economou [15]. The basic premises of this model were stated in detail in Refs. [15,16] as following: 1) The discharge was formed between two large-area parallel conductive electrodes, hence a 1D spatial approximation was permissible; 2) The particle flux was described by diffusion/drift approximation; 3) Electrons were assumed to have the Maxwell–Boltzman energy distribution function; 4) The ion temperature was assumed to be constant and equal to the neutral gas temperature. An energy equation for ions was not needed; 5) Magnetic field effects were not included. Based on these assumptions, the model equations were presented as follows:

$$\frac{\partial n_i}{\partial t} + \frac{\partial \Gamma_i}{\partial x} = S_i, \tag{1}$$

$$\Gamma_i = \pm n_i \mu_i E - D_i \frac{\partial n_i}{\partial x}, \tag{2}$$

$$\frac{\partial}{\partial t}\left(\frac{3}{2} n_e T_e\right) + \frac{\partial}{\partial_x}\left(\frac{5}{2}\Gamma_e T_e - K_e \frac{\partial T_e}{\partial_x}\right) + e\Gamma_e E + Q_{coll} = 0, \tag{3}$$

$$\varepsilon_0 \frac{\partial E}{\partial x} = e\left(\sum_i n_i - n_e\right). \tag{4}$$

With the drift-diffusion approximation [15,16], the continuity equation of plasma specie is given by Eqs. (1) and (2), in which subscript i represents electrons, ions and meta-stable species; n, Γ and S denote the number density, the flux density and the sources/losses of particles due to the reactions respectively; μ_i and D_i are the species mobility and diffusion coefficient; t and x represent the time and inter-electrode axial distance, respectively. Equation (3) is the energy transportation equation of electrons. Here e is the elementary charge, T_e is the electron temperature, Γ_e is the flux of electrons, K_e is the heat conduction coefficient and Q_{coll} is the energy loss arising from various reactions. The electric field across discharge gap is described with Poisson's equation as Eq. (4), where E, e, and ε_0 are the electric field, the elementary charge, and vacuum permittivity, respectively. The efficiency for the excitation of the level i by electron impact can be calculated by Eqs. (5)– (7) [17], where η_i is the efficiency for the excitation of the level i, w_i is the energy absorbed by one single event and n_j is the particle density of the gas component involved (CO_2, N_2, He). The power supplied to one electron by the electric field is read as $P_e(x)$. μ_e and k_i are electron mobility coefficient and species rate coefficient.

$$\eta_i = \frac{w_i n_j k_i(T_e)}{P_e}, \tag{5}$$

$$P_e(x) = e\mu_e E^2(x), \tag{6}$$

$$w_i(x) = e n_j[\mu_e + \mu_i] E^2(x). \tag{7}$$

In this study, it was supposed that all the energy supplied to the vibrational levels of N_2 was transferred to the asymmetric stretching mode of CO_2 molecules by collisions of the second kind. Thus, the efficiency for excitation of the upper laser level was a sum of $\eta_3 + \eta_{12}$.

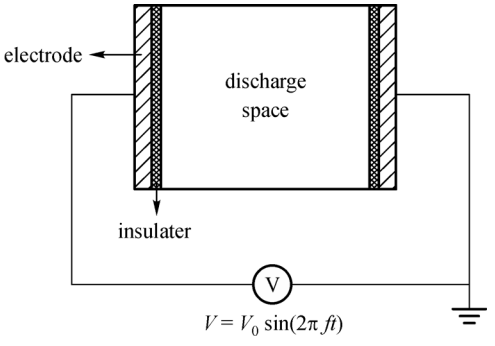

Fig. 1 Geometry of discharge system

On the boundary conditions, the electron temperature was set to be 0.5 eV and all species were set to zero. Because secondary electron emitted from the electrode surface has a relatively fixed energy value, the average electron energy of the fixed electrode surface can be set to 0.5 eV. In order to reduce the instability of numerical simulation and improve the efficiency of numerical

calculation, the initial values of the particle density and the average values of the electron energy on the whole discharge space were kept the same. The initial value of electric field was determined by the initial values of the density of charged particle and the applied voltage [15,18].

The discharge gases included CO_2, N_2 and He mixture at 120 mbar. The ratio of CO_2 was 5% of the total, and He was 67% while N_2 was 28%. A sinusoidal external voltage was applied to the discharge electrode. The voltage was 600 V, the electrode gap was 26 mm, the thickness of insulator was 3 mm, the relative permittivity of insulator was 7, and the driven frequency varied from 5 to 45 MHz. The density and temperature of the gas were assumed to be constant in time and uniform in space. The gas temperature was supposed to be 400 K. The initial value of the particles was given by $n_e = 10^7\ cm^{-3}$, and the density of other ions and neutral particles is set to 0. The time-averaged values are shown in Figs. 2–6. Before the calculation reaches to steady-state, self-consistent calculation was required to repeat about 1000 RF cycles. Based on the above description, Eqs. (1)–(4) were numerically solved under the initial conditions.

α-RF and γ-RF are two models of RF discharge. The result demonstrated that α-RF is more effective for excitation of glow discharge.

The α discharge pattern is often referred to as the low current discharge mode. This discharge is primarily maintained by ionization. The γ discharge is often called the high current discharge mode. It is mainly caused by the second electron emission.

In α-RF discharge, the plasma is weakly ionized under medium-pressure and medium-frequency. The processes of electron-electron collision, electron-ion collision, super elastic collision and the meta-stable processes could be neglected [19]. So, the main reaction in glow discharge with CO_2/He/N_2 mixture plasma is given in Table 1 and the coefficients of reaction in CO_2 are obtained from Refs. [20–22]. The coefficients of reactions in N_2 and He are provided by Refs. [23] and [24], respectively.

3 Results and discussion

The electron densities under different frequencies were shown in Fig. 2, it was indicated variation in electron density can be considered as a function of excited frequency. In Fig. 2, the position represents the spacing between the two electrodes. From Fig. 2, it can be observed that the electron density distribution is symmetric in general and the maxima of electron density occurs at sheath region, whereas the electron density in plasma bulk region is relatively smaller, and the distribution of electron density drifts up as the excitation frequency increases. These findings can be used to explain why the most luminous layer appears near the two electrodes, whereas the luminosity in the central discharge area (plasma bulk region) is relatively weaker, and these results were experimentally observed by some researchers [12,25,26].

These two different discharge modes have been verified in RF discharge [27]. One is α mode and the density of discharge current is relatively low, the other terms is γ mode, and the density of discharge current is relatively high [28,29]. Figure 3 shows the current amplitude with different excitation frequency. On the boundary conditions, the 600 V voltage was loaded at the electrodes. This means that a constant power is adopted in this numerical simulation. That is to say, we just considered effects of the excitation frequency on discharge at a constant power in this study. It was found in Fig. 3 that the current amplitude increase linearly with the excitation frequency

Table 1 Collision reactions in the simulation

No.	process	notation
1	excitation of the bending mode (010) in CO_2	$e + CO_2 \rightarrow e + CO_2^{V010}$
2	excitation of the lower laser level (020 + 100) in CO_2	$e + CO_2 \rightarrow e + CO_2^{V020+100}$
3	excitation of the asymmetric stretching mode (001) in CO_2	$e + CO_2 \rightarrow e + CO_2^{V001}$
4	electronic excitation of CO_2	$e + CO_2 \rightarrow e + CO_2^{*}$
5	dissociative attachment in CO_2	$e + CO_2 \rightarrow CO + O^{-}$
6	ionization of CO_2	$e + CO_2 \rightarrow 2e + CO_2^{+}$
7	elastic collisions of He with electrons	$e + He \rightarrow e + He$
8	electronic excitation of He	$e + He \rightarrow e + He^{*}$
9	ionization of He	$e + He \rightarrow 2e + He^{-}$
10	elastic collisions of N_2 with electrons	$e + N_2 \rightarrow e + N_2$
11	ionization of N_2	$e + N_2 \rightarrow 2e + N_2^{+}$
12	excitation of vibration mode in N_2	$e + N_2 \rightarrow e + N_2^{*Vib}$
13	excitation of rotation mode in N_2	$e + N_2 \rightarrow e + N_2^{*Rot}$

ranging from 5 to 15 MHz, then the slower growth of current amplitude occurs as the excitation frequency varying from 15 to 25 MHz, finally the current amplitude obviously rises with the excitation frequency between 25 and 45 MHz. The variation of the current amplitude was relatively small when the excitation frequency increased from 5 to 45 MHz. The α -> γ discharge mode transition has not been seen. Although the growth rate of discharge current has a drop when the frequency increases from 15 to 25 MHz, the electron density is still growing with the increasing excitation frequency. Figures 2 and 4 respectively show the growth rate of electron density and electron production rate are relatively low in the frequencies ranging from 15 to 25 MHz. That is to say, electronic shock and collision are relatively weak in that frequency range and there are relatively few electron to maintain the discharge. Therefore, the growth rate of discharge current decrease in the frequency varying from 15 to 25 MHz. Moreover, it was seen in Fig. 2, as the excitation frequency increases, the distribution of electron density grows up smoothly. This distribution is similar to the photograph of the RF plasma operating in the α mode in Ref. [27]. Thus, we deduced the discharge is α mode.

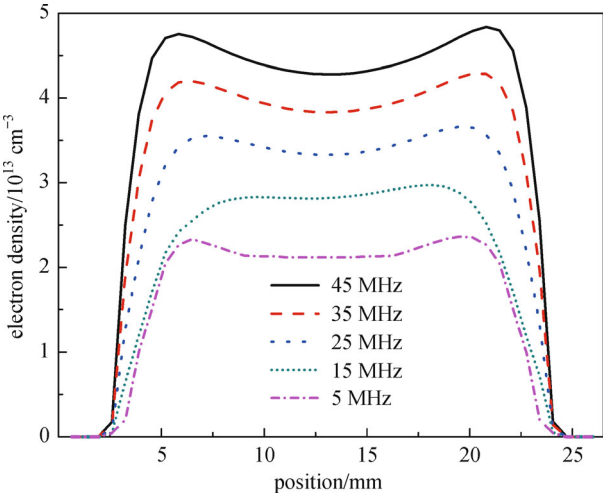

Fig. 2 Electron density versus excitation frequency in spatial profiles

In order to provide the discharge operating in α mode, spatial profiles of the electron production rate with different frequencies were simulated and the results were shown in Fig. 4. It shows that electron production exists in whole discharge region including sheath region and plasma bulk region.

The sheath region is a layer in a plasma, which has a greater density of ions. The plasma bulk region contains a large number of positive and negative charged particles; the positive and negative charge density is equal in this region.

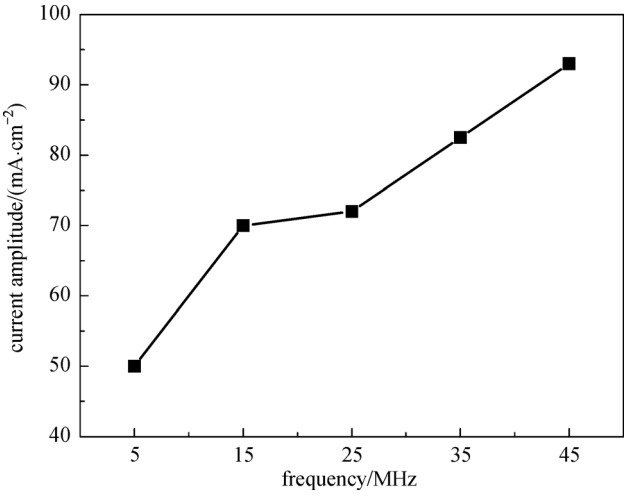

Fig. 3 Current amplitude versus excitation frequency

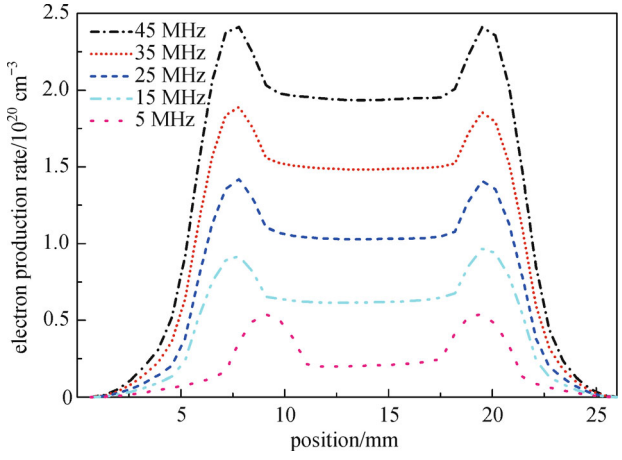

Fig. 4 Electron production rate versus excitation frequency in spatial profiles

The spatial profile of gas ionization is saddle shape and this profile complies with α mode discharge theory [26,30]. What's more, in high driven frequency, the α mode discharge is a more favorable discharge model [31]. So, we deduce the gas is discharged in α mode from 5 to 45 MHz.

To further investigate the underlying physics of the electron production rate, the spatial distributions of electric field and electron temperature at five different excitation frequencies were also studied, we found that the electric field near the electrode at 5 MHz of excitation frequency was over 2.7 kV/cm in sheath region; the thickness of this region was around 4 mm. As the frequency increased to 45 MHz, the electric field in the sheath region was only about 2 kV/cm, and the thickness of sheath decreased from 4 to 3 mm. As seen in Fig. 5, the electric field is stronger in sheath, and more electrons can gain more energy from the electric field to reach ionization energy. The calculated results indicated that the increasing frequency will reduce

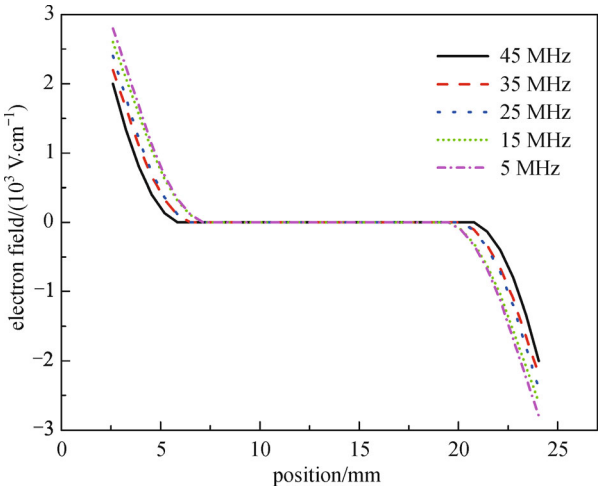

Fig. 5 Electric field versus excitation frequency in spatial profiles

the electric fields, compress the sheath region, and provide a more stable discharge. The thinner sheath region means that there is a larger effective excitation area (plasma bulk region) for use, and a higher excitation efficiency for the upper laser level, all of which are helpful for laser power extraction and consistent with Refs. [12]. and [13]. It is clearly shown in Fig. 6 that electron temperature decreases with the excitation frequency, and the electron temperature is much lower in the bulk plasma region than that in the sheath region. This is probably due to the electric field in the sheath region is higher than that in the bulk plasma region. Electron collision in the sheath region can be more intense and previously related experiments were also in line with this deduction [14].

The higher the particle density of the upper laser level is, the excitation efficiency gets higher. The excitation of this level is produced by two ways. One is direct electron impact with CO_2 molecules and the other is contributed by energy transfer by the second electron collisions of with vibration excited N_2 molecules. However, many other energy levels are also excited by a loss of energy with respect to laser operation. For lower electron energies, it is electronic excitation which is main excitation of bending modes in CO_2. Hence, we also simulated the distribution of maximum particle density and the efficiency for the excitation with different frequencies, results were shown in Figs. 7 and 8. It is obviously seen that the density of CO_2^{V001} and N_2^{*Vib} grows with the excited frequency. Moreover, there are larger effective excitation area and higher excitation efficiency for the upper laser level by increasing the frequency. These are beneficial for laser power extraction. This conclusion is validated by Refs. [12] and [13].

When the excitation frequency is increased, the sheath region is compressed (see Fig. 2).The more electrons are brought out from the compressed sheath region. These electrons are contributed to the plasma bulk region and

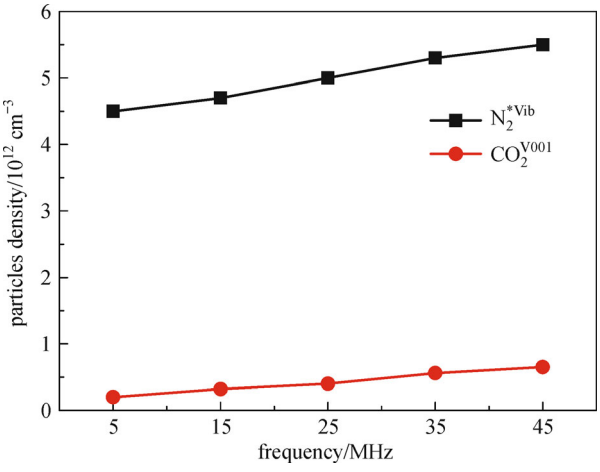

Fig. 7 Maximum density of main particles versus excitation frequency

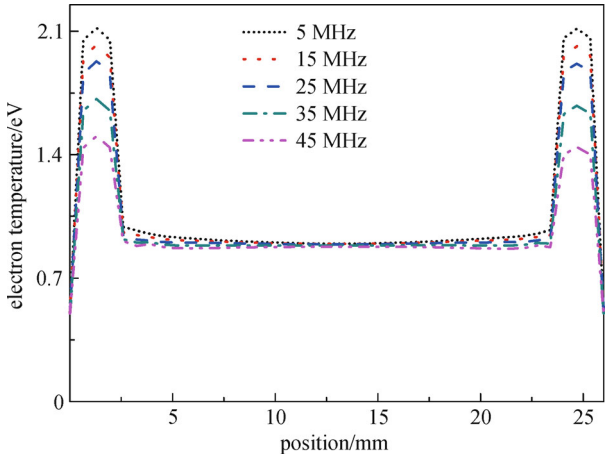

Fig. 6 Electron temperature versus excitation frequency in spatial profiles

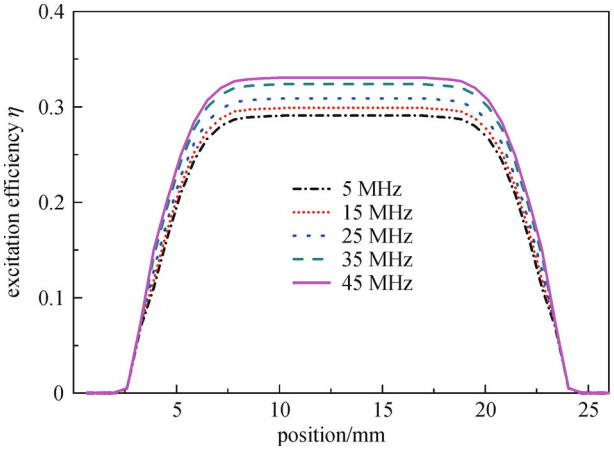

Fig. 8 Excitation efficiency versus excitation frequency in spatial profiles

more electrons engage in reactions in this region. Hence, the reaction can gain higher particle density with modulating the excited frequency and the density of CO_2^{V001} and N_2^{*Vib} is important to get higher excitation efficiency for the upper laser level.

4 Conclusions

1D self-consistent fluid model was used to describe the discharges in the RF excited fast axial flow CO_2 laser at different RF. The effect of excitation frequency on such characteristic parameters as the spatial distributions of electron density, electric field, electron production rate, as well as electron temperature and the distribution of the maximum particle density and current amplitude has been evaluated. The results indicate that with the increasing excitation frequency, the discharge is in α mode. Moreover, the higher particles density can be obtained by modulating the excitation frequency. Furthermore, the result explains satisfactorily some electrical properties of the discharges.

References

1. Sublemontier O, Lacour F, Leconte Y, Herlin-Boime N, Reynaud C. CO_2 laser-driven pyrolysis synthesis of silicon nanocrystals and applications. Journal of Alloys and Compounds, 2009, 483(1–2): 499–502
2. Comparat D. A study of molecular cooling via Sisyphus processes. Physical Review A, 2014, 89(4): 043410
3. Niziev V G, Grishaev R V, Panchenko V Y. Multipass modes in an open resonator. Laser Physics, 2015, 25(2): 023001
4. Zhao J, Li B, Zhao H, Wang W, Hu Y, Liu S, Wang Y. Generation of azimuthally polarized beams in fast axial flow CO_2 laser with hybrid circular subwavelength grating mirror. Applied Optics, 2014, 53 (17): 3706–3711
5. Maiorov S A, Kodanova S K, Dosbolayev M K, Ramazanov T S, Golyatina R I, Bastykova N K, Utegenov A U. The role of gas composition in plasma-dust structures in RF discharge. Physics of Plasmas, 2015, 22(3): 033705
6. Voloshin D, Kovalev A, Mankelevich, Proshina O, Rakhimova T, Vasilieva A. Evaluation of plasma density in RF CCP discharges from ion current to Langmuir probe: experiment and numerical simulation. Evaluation Physical Journal D, 2015, 69(23): 1–9
7. Chen F F, Evans J D, Zawalski W. Calibration of Langmuir probes against microwaves and plasma oscillation probes. Plasma Sources Science & Technology, 2012, 21(5): 055002
8. Turner M M, Derzsi A, Donkó Z, Eremin D, Kelly S J, Lafleur T, Mussenbrock T. Simulation benchmarks for low-pressure plasmas: capacitive discharges. Physics of Plasmas, 2013, 20(1): 013507
9. Wester R, Seiwert S. Numerical modelling of RF excited CO_2 laser discharges. Journal of Physics D, Applied Physics, 1991, 24(8): 1371–1375
10. Wang Y, Chen Q, Xu Q Y. Numerical modeling of RF-excited plasma in coaxial CO_2 lasers. Optics Communications, 1999, 160 (1–3): 86–91
11. Zhang X, Wang X, Li G, He F, Jiao J, Lu Y. Theoretical research of α-RF discharge in slab oxygen iodine lasers. Proceedings of High-Power Lasers and Applications IV, 2007, 6823: 68230Q
12. He D, Hall D R. Frequency dependence in RF discharge excited waveguide CO_2 lasers. IEEE Journal of Quantum Electronics, 1984, 20(5): 509–514
13. Vidaud P, He D, Hall D R. High efficiency RF excited CO_2 laser. Optics Communications, 1985, 56(3): 185–190
14. Vidaud P, Hall D R. Effect of xenon on the electron temperatures of RF discharge CO_2 laser gas mixtures. Journal of Applied Physics, 1985, 57(5): 1757–1758
15. Lymberopoulos D P, Economou D J. Fluid simulations of glow discharges: effect of metastable atoms in argon. Journal of Applied Physics, 1993, 73(8): 3668–3679
16. Liu X M, Song Y H, Wang Y N. Driving frequency effects on the mode transition in capacitively coupled argon discharges. Chinese Physics B, 2011, 20(6): 065205
17. Schroder K. Theoretical modelling of RF-excited laser plasmas. Proceedings of the Society for Photo-Instrumentation Engineers, 1989, 1031: 90–97
18. Shang W, Wang D, Zhang Y. Radio frequency atmospheric pressure glow discharge in α and γ modes between two coaxial electrodes. Physics of Plasmas, 2008, 15(9): 093003
19. Raizer Y P, Shneider M N, Yatsenko N A. Radio-Frequency Capacitive Discharges. Florida: CRC, 1995, 247–258
20. Lowke J J, Phelps A V, Irwin B W. Predicted electron transport coefficients and operating characteristics of CO_2-N_2-He laser mixtures. Journal of Applied Physics, 1973, 44(10): 4664–4671
21. Schulz G J. Vibrational excitation of N_2, CO, and H_2 by electron impact. Physical Review, 1964, 135(4A): A988–A994
22. Newman L A, Detemple T A. Electron transport parameters and excitation rates in N_2. Journal of Applied Physics, 1976, 47(5): 1912–1915
23. Cosby P C. Electron-impact dissociation of nitrogen. Journal of Chemical Physics, 1993, 98(12): 9544–9553
24. Surendra M. Radiofrequency discharge benchmark model comparison. Plasma Sources Science & Technology, 1995, 4(1): 56–73
25. Bhagat M S, Biswas A K, Rana L B, Kukreja L M. Impedance matching in RF excited fast axial flow CO_2 laser: the role of the capacitance due to laser head. Optics & Laser Technology, 2012, 44 (7): 2217–2222
26. He D, Baker C J, Hall D R. Discharge striations in RF excited waveguide lasers. Journal of Applied Physics, 1984, 55(11): 4120–4122
27. Yang X, Moravej M, Nowling G R, Babayan S E, Panelon J, Chang J P, Hicks R F. Comparison of an atmospheric pressure, radio-frequency discharge operating in the α and γ modes. Plasma Sources Science & Technology, 2005, 14(2): 314–320
28. Moon S Y, Rhee J K, Kim D B, Choe W. α, γ, and normal, abnormal glow discharge modes in radio-frequency capacitively coupled discharges at atmospheric pressure. Physics of Plasmas, 2006, 13(3): 033502
29. Liu D, Iza F, Kong M G. Evolution of the light emission profile in radio-frequency atmospheric pressure glow discharges. IEEE Transactions on Plasma Science, 2008, 36(4): 952–953

30. Vitruck P P, Baker H J, Hall D R. The characteristics and stability of high power transverse radio frequency discharges for waveguide CO_2 slab laser excitation. Journal of Physics D, Applied Physics, 1992, 25: 1767
31. Zhang Y, Cui S. Frequency effects on the electron density and α–γ mode transition in atmospheric radio frequency discharges. Physics of Plasmas, 2011, 18(8): 083509

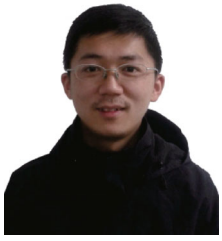

Heng Zhao is a Ph.D. candidate in the School of Optical and Electronic Information of Huazhong University of Science and Technology in Wuhan, Hubei, China. He received his B.S. degree from Huazhong University of Science and Technology. His current research interests include high power gas laser, integration of high power laser processing system and radio frequency (RF) power amplifier.

Bo Li obtained his B.S., M.S. and Ph.D. degrees from Huazhong University of Science and Technology in 2000, 2003 and 2010, respectively. Currently, he is a lecturer of the School of Optical and Electronic Information of Huazhong University of Science and Technology. His research fields are: high-power lasers and laser processing.

Wenjin Wang is a Ph.D. candidate in the School of Optical and Electronic Information of Huazhong University of Science and Technology in Wuhan, Hubei, China. His interests include research on a high-power CO_2 laser system design and optimization, gas discharge stability, and the kinetic modeling.

Yi Hu is a Ph.D. candidate in the School of Optical and Electronic Information of Huazhong University of Science and Technology in Wuhan, Hubei, China. She received her B.S. degree from Huazhong university of Science and Technology. Her current research focuses on laser physics, laser optics, and high power laser industrial application.

Youqing Wang is a Professor and doctoral advisor, who has long been engaged in basic research on a high-power CO_2 laser and applied research on laser processing material. Wang is with the College of Optoelectronic Science and Technology, Huazhong University of Science and Technology, Wuhan, China.